

# Steps toward the power spectrum of matter. I. The mean spectrum of galaxies

J. Einasto<sup>1</sup>, M. Einasto<sup>1</sup>, E. Tago<sup>1</sup>, A. A. Starobinsky<sup>2</sup>, F. Atrio-Barandela<sup>3</sup>, V. Müller<sup>4</sup>,  
A. Knebe<sup>4</sup>, P. Frisch<sup>5</sup>, R. Cen<sup>6</sup>, H. Andernach<sup>7</sup> and D. Tucker<sup>8</sup>

## ABSTRACT

We calculate the mean power spectrum of all galaxies using published power spectra of galaxies and clusters of galaxies. On small scales we use the power spectrum derived from the 2-dimensional distribution of APM galaxies, since this sample is not influenced by redshift distortions and is the largest and deepest sample of galaxies available. On large scales we use power spectra derived from 3-dimensional data for various galaxy and cluster samples which are reduced to real space and in amplitude to the power spectrum of APM galaxies. We find that available data indicate the presence of two different populations in the nearby Universe. Clusters of galaxies sample a relatively large region in the Universe where rich, medium and poor superclusters are well represented. Their mean power spectrum has a spike at wavenumber  $k = 0.05 \pm 0.01 \ h \text{ Mpc}^{-1}$ , followed by an approximate power-law spectrum of index  $n \approx -1.9$  towards small scales. Some galaxy surveys (APM 3-D, IRAS QDOT, and SSRS+CfA2 130 Mpc) have similar spectra. The power spectrum found from LCRS and IRAS 1.2 Jy surveys is flatter around the maximum, which may represent regions of the Universe with medium-rich and poor superclusters. Differences in power spectra for these populations may partly be due to the survey geometries of the datasets in question and/or to features of the original data analysis.

---

<sup>1</sup>Tartu Observatory, EE-2444 Tõravere, Estonia

<sup>2</sup>Landau Institute for Theoretical Physics, Moscow 117334, Russia

<sup>3</sup>Física Teórica, Universidad de Salamanca, 37008 Spain

<sup>4</sup>Astrophysical Institute Potsdam, An der Sternwarte 16, D-14482 Potsdam, Germany

<sup>5</sup>Göttingen University Observatory, Geismarlandstr. 11, D-37083 Göttingen, Germany

<sup>6</sup>Department of Astrophysical Sciences, Princeton University, Princeton, NJ 08544, USA

<sup>7</sup>Depto. de Astronomía, IFUG, Apdo. Postal 144, C.P. 36000 Guanajuato, Gto., Mexico

<sup>8</sup>Fermilab, MS 127, Box 500, Batavia, IL 60510, USA

*Subject headings:* cosmology: large-scale structure of the universe – cosmology: observations – galaxies: formation

## 1. Introduction

The power spectrum of matter is one of the most important statistics to describe the large-scale structure of the Universe. If the distribution of density inhomogeneities is Gaussian then the power spectrum characterizes the distribution of matter (in a statistical sense) completely. During the last decade considerable efforts have been devoted to determining this function empirically from the distribution of galaxies and clusters of galaxies. These studies have shown that on small scales the power spectrum in real space can be satisfactorily expressed by a power law with an index somewhere between  $-2$  and  $-1.5$ . On larger scales the spectrum turns over reaching a maximum on scales of  $100 - 150 h^{-1} \text{ Mpc}$  (we use a Hubble constant of  $100 h \text{ km s}^{-1} \text{ Mpc}^{-1}$ ).

The exact location of the maximum, its amplitude and shape are not well determined yet. The deep pencil-beam redshift survey of Broadhurst et al. (1990) indicates the presence of a sharp spike at a scale of  $l = 128 h^{-1} \text{ Mpc}$  or wavenumber  $k = 2\pi/l = 0.05 h \text{ Mpc}^{-1}$ . Power spectra of Abell-ACO clusters of galaxies (Einasto et al. 1997a, hereafter E97a, Retzlaff et al. 1998, hereafter R98), and APM clusters (Tadros et al. 1998, T98) also indicate a rapid turnover from a spectrum with negative slope on galactic scales to a spectrum with positive slope; the turnover occurs at a high amplitude on a scale similar to the scale of the spike found by Broadhurst et al. . But not all power spectra obtained from galaxy surveys support this picture. Some data show a much flatter spectrum near the maximum: the 3-D spectrum analysis of the Las Campanas Redshift Survey (LCRS; Lin et al. 1996, hereafter LCRS3d), and the IRAS surveys discussed by Tadros and Efstathiou (1995, hereafter TE95).

Our main goal is to determine the mean matter power spectrum using all available data. This will be done in three steps. First, we derive the mean power spectrum of galaxies that best agrees with available observations and determine its main parameters (present Paper). By “the mean power spectrum of galaxies” we understand the spectrum of a population which includes all galaxies in real space in a large volume (fair sample). Second, we investigate the biasing phenomenon and develop a method to reduce the galaxy power spectrum to matter (Einasto et al. 1999a, Paper II). The method is based on the assumption that the structure evolution in the Universe is due to gravity; in this case galaxy formation is essentially a threshold process. We find a relation between the biasing parameter and the fraction of mass in clustered objects (galaxies). We use numerical simulations to follow the flow of matter from low-density to high-density regions. In these simulations, we identify the current epoch by comparing the  $\sigma_8$  parameter of the spectrum with its observed value. Finally, in the third step we determine the power spectrum of matter in the linear regime and compare it with different model predictions (Einasto et al. 1999b, Paper III). This approach is similar to Peacock & Dodds (1994) but, in addition, we also determine the primordial

matter power spectrum.

The present paper is organized as follows. In Section 2, we describe the power spectra we shall use in our analysis. In Section 3, we discuss why different catalogs give rise to different power spectra. In Section 4, we derive the mean power spectrum by combining the information from different catalogs, and determine the parameters that define the power spectrum empirically such as its slope, amplitude, and the shape parameter. In Section 5 we check this spectrum for consistency using recent determinations of the correlation function for various galaxy and cluster samples. Finally, we draw our main conclusions.

## 2. Power spectra from galaxy and cluster data

In this article, our goal is to derive the mean power spectrum of all galaxies over a wide range of scales. Our main assumption is that there exists one single power spectrum that characterizes the distribution of a general population of all galaxies (including giant and dwarf galaxies, and galaxies of all morphological types) in a large volume (fair sample of the Universe). Real galaxy populations are subsamples of this general galaxy population, selected in a subvolume and in certain limited luminosity and/or morphological type intervals of the fair sample. Our practical task is to reduce power spectra determined from limited galaxy populations to the fair sample. The mean power spectrum shall be determined in or reduced to real space.

We use the following published power spectra: the SSRS+CfA2 130 Mpc/h volume-limited survey for  $M_B < -20.3 + 5 \log h$  by da Costa et al. (1994, hereafter dC94), the Stromlo-APM “1-in-20” redshift survey of APM galaxies (Tadros and Efsthathiou 1996, hereafter TE96), the power spectrum analysis of the Las Campanas Redshift Survey (3-D spectral analysis by LCRS3d, and 2-D analysis by Landy et al. (1996), hereafter LCRS2d), and two IRAS surveys, the 1.2 Jy survey and the “1-in-6” QDOT survey (Saunders, Rowan-Robinson & Lawrence 1992), discussed by TE95, and by Peacock (1997, hereafter P97). For comparison we use power spectra of fainter galaxies: the CfA redshift survey (Vogeley et al. 1992, Park et al. 1994), the SSRS+CfA2 101 Mpc/h volume-limited survey for  $M_B < -19.7 + 5 \log h$  by dC94; and power spectra found by Gramann & Einasto (1992, hereafter GE92) for galaxies in the the Local, Coma and Perseus superclusters. When this study was finished we received a preprint of the power spectrum analysis of the Durham/UKST 1 in 3 Galaxy Redshift Survey by Hoyle et al. (1998). The power spectrum found for this survey is very similar to the spectrum of the Stromlo-APM survey by TE96, which lies close to our mean power spectrum  $P_{HD}(k)$  (see below). This provides an important confirmation to one of our conclusions that power spectra of galaxy samples which cover a large volume are close to power spectra of

cluster samples, thus these samples can be considered as fair samples of the Universe.

In addition, we use results obtained from the APM two-dimensional galaxy distribution (Maddox et al. 1996 and references therein). This galaxy catalog is not influenced by redshift distortions (Kaiser 1987, Gramann et al. 1993) and, therefore, is of special value to determine the power spectrum in real space. The problem consists in finding the full three-dimensional power spectrum from two-dimensional data. Recently, Peacock (P97) and Gaztañaga & Baugh (1998, GB98) elaborated a procedure to use the APM Galaxy Survey. Their results showed a very good mutual agreement; the shapes of spectra are almost identical, but amplitudes are slightly different. We include the mean of these two spectra in our analysis.

The power spectra of Abell-ACO clusters (Abell 1958, Abell, Corwin and Olowin 1989) were determined by E97a and R98; for APM clusters (Dalton et al. 1997 and references therein) by T98. The power spectra of clusters are similar in shape to those of galaxies (in the range of scales not distorted by peculiar velocities) except that the cluster power spectra are enhanced in amplitude:

$$P_{cl}(k) = b_{cl}^2 P_{gal}(k), \quad (1)$$

where  $k$  is the wavenumber expressed in units of  $h \text{ Mpc}^{-1}$ , and  $b_{cl}$  is the bias factor of clusters relative to galaxies. We shall investigate the possible error of this reduction below.

Power spectra determined from galaxy and cluster surveys are plotted in Figure 1. We use the normalization of the power spectrum

$$P(k) = 2\pi^2 k^{-3} \Delta^2(k), \quad (2)$$

where  $\Delta^2(k)$  is the dimensionless power spectrum (see Peacock & Dodds 1994).

An inspection of our Figure 1 (and a similar Figure by Vogeley (1998)) indicates that, while different spectra obtained from different surveys agree with each other in the power law behavior on small scales, the shape and location of the maximum is not uniquely determined. The spectra of clusters and APM galaxies (TE96) have a well-determined sharp maximum, whereas IRAS and LCRS galaxies yield a low-amplitude maximum; cluster samples indicate a rapid decline in amplitude for  $k \leq 0.05 h \text{ Mpc}^{-1}$  while most galaxy samples show a much more modest decrease. The position of the maximum for APM clusters lies at  $k \approx 0.03 h \text{ Mpc}^{-1}$ , for Abell-ACO clusters and APM 3-D galaxies at  $k \approx 0.05 h \text{ Mpc}^{-1}$ , and for LCRS galaxies at  $k \approx 0.06 h \text{ Mpc}^{-1}$ .

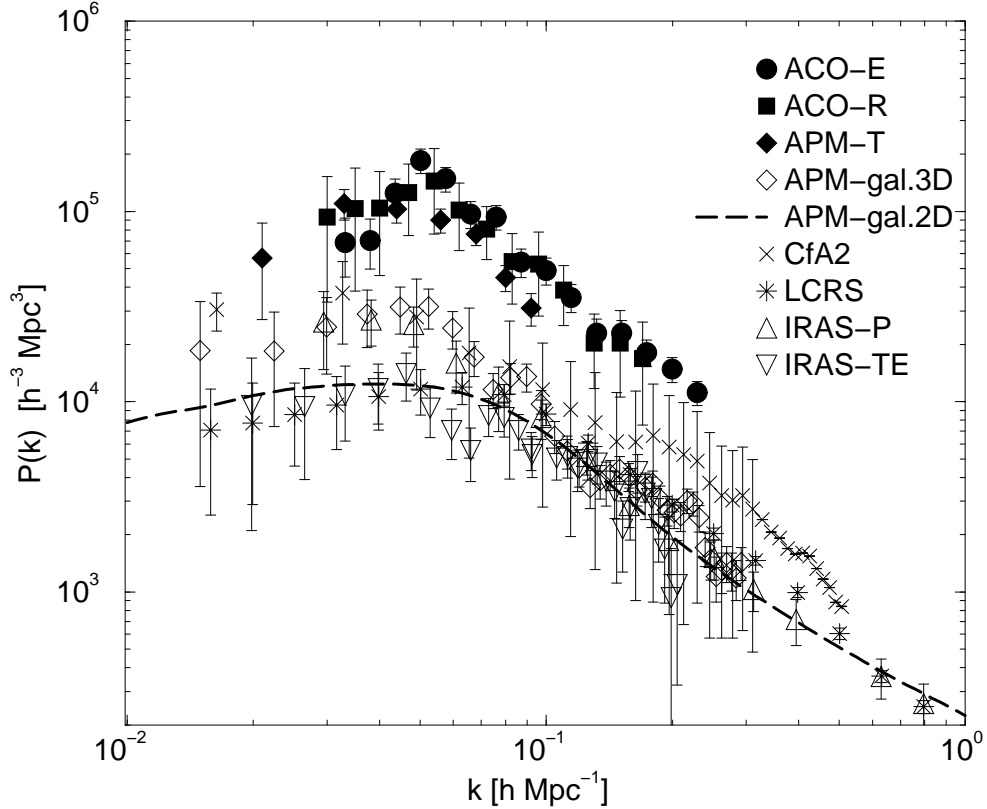


Fig. 1.— Observed power spectra of galaxies and clusters of galaxies. ACO-E and ACO-R are spectra for Abell-ACO clusters as derived by E97 and R98; APM-T is the spectrum of APM clusters according to TE98; APM-gal.3D and APM-gal.2D are spectra of APM galaxies found from 3-D and 2-D data by TE96 and by P97 and GB98, respectively; CfA2 is the spectrum of the SSRS+CfA2 130 Mpc/h sample by dC94, LCRS is the spectrum of the LCRS according to LCRS3d; IRAS-P and IRAS-TE are spectra of IRAS galaxies found by P97 and TE95.

### 3. Analysis of observed power spectra

In the previous Section we pointed out the discrepancies between the power spectra obtained from different galaxy and cluster surveys. In this Section we intend to clarify the source of these discrepancies and to analyze which spectra correspond better to the actual power spectrum of all galaxies (for a fair sample of the Universe).

#### 3.1. Spectra of galaxies in high- and low-density regions

A striking feature in Figure 1 is the difference between the power spectrum of IRAS galaxies (as reduced by TE95) and that of Abell-ACO clusters. It is well known that IRAS

galaxies are under-represented in high-density regions. To understand the origin of this discrepancy and its relation to the type of galaxy in the survey, we have performed numerical N-body simulations. Since spatial resolution was crucial, we performed a 2-D analysis. We used a double-power law initial power spectrum, which is a simple approximation of observed spectra of galaxies and clusters of galaxies with a spike at the maximum (Frisch et al. 1995)

$$P(k) = \begin{cases} Ak^n, & k \leq k_0; \\ Ak_0^n(k/k_0)^m, & k > k_0, \end{cases} \quad (3)$$

where  $n$  is the power index on large scales,  $m$  is the power index on small scales and is negative, and  $k_0$  is the transition wavenumber. In our 2-D simulations we used indices  $n = 2$  and  $m = -1$ ; in the 3-D case these indices correspond to  $n = 1$  and  $m = -2$  on large and small scales, respectively. The turnover scale was taken to be 1/4 of the simulation box size. We used a box size of  $L = 512 \ h^{-1}$  Mpc. The present epoch was identified using an rms density dispersion of  $\sigma_1 = 4$  on a scale of  $1 \ h^{-1}$  Mpc, which corresponds to a variance of approximately  $\sigma_8 = 0.9$  on a scale of  $8 \ h^{-1}$  Mpc (Einasto et al. 1994a, hereafter E94). We use a critical density universe, and express densities  $\varrho$  in units of the critical (mean) density. A top-hat smoothing over  $1 \ h^{-1}$  Mpc is used to determine the density field. This procedure reproduces the distribution of dark matter as accurately as possible. Dark matter forms halos around galaxies and groups with a characteristic scale of  $\sim 1 \ h^{-1}$  Mpc (E94).

A density value was assigned to each particle by interpolating the density field at the particle location. We assume that particles in the simulation belong to different populations according to their environment, i.e. that galaxy samples of various environment, morphology and luminosity can be approximated by particles in numerical simulations chosen in certain threshold density intervals. We shall discuss this assumption and the relation between real and simulated galaxies in more detail in Paper II. We call all particles with low density values ( $\varrho < \varrho_0$ ) *void particles*. The remaining particles are clustered and form systems of various richness; we call these clustered particles *galaxies*, actually they represent dark matter in galaxies and galaxy systems. Particles with very high density values ( $\varrho \geq \varrho_{cl}$ ) belong to clusters or groups, and particles with intermediate density values ( $\varrho_0 \leq \varrho < \varrho_{cl}$ ) shall be called *field galaxies*. Here  $\varrho_0$  and  $\varrho_{cl}$  are threshold densities which separate void particles from galaxies, and field galaxies from cluster galaxies, respectively.

Figure 2 shows power spectra found for this simulation. Here we have used threshold densities  $\varrho_0 = 1$  and  $\varrho_{cl} = 5$ . In the present paper these values serve as illustrations; their exact values can be determined using various tests (clustering properties as applied by E94, or hydrodynamical simulations as in Cen and Ostriker 1992, 1998). Obviously, the power spectrum of all galaxies ( $\varrho \geq 1$ ) is similar to the matter power spectrum, but has a

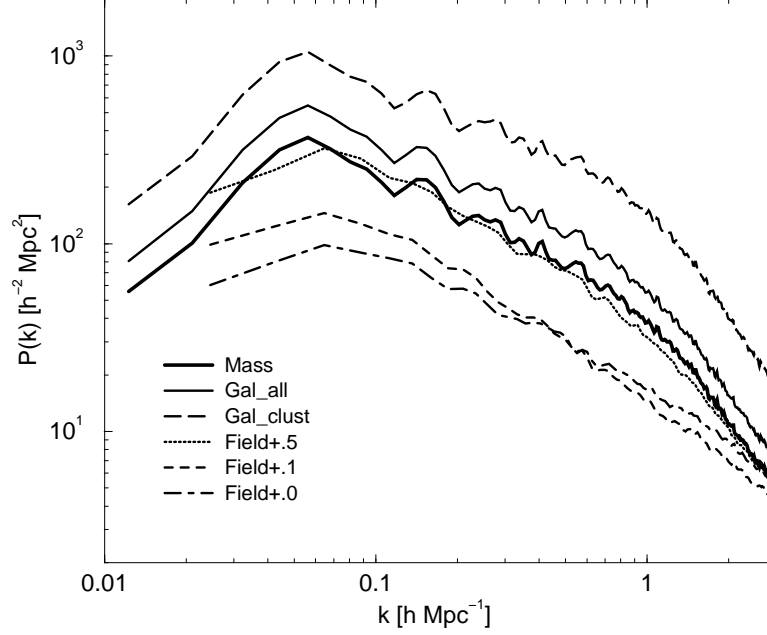


Fig. 2.— Power spectra of simulated galaxies. The solid bold line shows the spectrum derived for all test particles (the matter power spectrum); various dashed and dotted lines give the power spectrum of all galaxies, clustered galaxies in high-density regions, and galaxies in the intermediate density regions (simulated field galaxies). The sample Field+.0 consist of galaxies between threshold densities  $1 \leq \varrho < 5$  only; samples Field+.1 and Field+.5 contain also 10 % and 50 % of galaxies selected randomly from cluster galaxies with  $\varrho \geq 5$ .

higher amplitude. The power spectrum of field galaxies in the intermediate density range ( $1 \leq \varrho < 5$ ) has a lower amplitude than that of the sample of all galaxies; it is even lower than the amplitude of the matter power spectrum. Furthermore, the shape of the spectrum is different as well: the maximum of the spectrum is flatter, and the power index on small scales is lower.

The population of all clustered particles (i.e. galaxies) differs from the whole mass population in a simple way – it does not include non-clustered particles in low-density regions (i.e. the void population). Power spectra are defined by the density contrast, which leads to the formula

$$P_m(k) = F_c^2 P_c(k), \quad (4)$$

where  $P_m(k)$  and  $P_c(k)$  are power spectra of mass and clustered particles, respectively, and  $F_c$  is the fraction of matter in clustered particles (galaxies). The formula is exact if the distribution of matter in low-density regions (voids) is homogeneous (Paper II). In practice it can be used for a wide range of threshold densities  $\varrho_0$  to divide the matter into low- and high-



density regions. The form of the power spectrum of clustered particles remains similar to that of all particles, only its amplitude has changed according to eqn. (4). Luminous galaxies are more clustered than faint ones; thus, varying the threshold density, one can simulate galaxy samples of different absolute magnitude limit, and galaxies in clusters or groups. Thus this formula can be used to reduce power spectra of galaxies of various luminosity to the spectrum of all galaxies, and the spectrum of all galaxies to that of all matter. We shall discuss possible errors of this reduction in Section 4.7 below.

The shape of the power spectrum is conserved in the case when only particles or galaxies in low-density regions are excluded by a certain threshold density or luminosity limit. If samples of particles or galaxies are not complete in high-density (luminous galaxy) regions then the shape of the power spectrum is not conserved (see the next subsection). To simulate qualitatively different catalogs we chose galaxies in low- and medium-density regions as representatives of IRAS galaxies, or as galaxies in poor superclusters (Einasto et al. 1997b, 1997c, hereafter E97b, E97c). In contrast to galaxies in high-density regions, the power spectrum of galaxies in intermediate density regions is not related to the matter power spectrum in a simple way. Thus, it is not easy to reduce the power spectra of galaxies in intermediate density regions to all galaxies or to all matter distribution. But it is clear that a population, with a more homogeneous distribution than that of all galaxies, has a power spectrum which lies between the spectrum of a homogeneous population (a flat spectrum of low amplitude) and the spectrum of all clustered particles.

The main conclusions obtained from our simulation are the following. *Exclusion of dark matter particles or galaxies from low-density regions raises only the amplitude of the power spectrum in real space without changing its shape*, whereas *the exclusion of galaxies from high-density regions decreases the amplitude and changes the shape of the power spectrum*. In the first case we can reduce data to form a mean power spectrum characteristic for all galaxies using eqn. (4); in the second case the shape of the power spectrum is not conserved and the reduction of the power spectrum is complicated, thus it is better to consider the medium-density population and its power spectrum separately. These results are based on the assumption that galaxy samples can be approximated by particles in numerical simulations chosen in certain threshold density intervals (see Section 4.7 and Paper II for a detailed analysis of this assumption).

### 3.2. The influence of superclusters on IRAS data

TE95 analyzed the power spectra of two IRAS surveys, the 1.2 Jy survey and the “1-in-6” QDOT survey. They find that the spectrum of the QDOT survey has a higher amplitude,

and, if galaxies of the Hercules supercluster are excluded, then both samples of IRAS galaxies yield a similar power spectrum with a rather low amplitude, flat maximum.

We can consider intermediate-density (field) galaxies as representing IRAS galaxies. Figure 2 shows that, if we exclude all galaxies in high-density regions from our sample (this sample is marked Field+.0 in Figure 2), then the power spectrum of this intermediate-density population has an amplitude near the maximum which is lower, by almost a factor of 10, than the amplitude of the spectrum of all galaxies. The shape of this simulated field galaxy spectrum is also different: the maximum is much flatter. Actually IRAS galaxies are not completely absent in clusters, they are only under-represented. To simulate this behavior we have formed a second simulated population of field galaxies which includes all galaxies of the previous field galaxy sample, and a fraction (10 %) of cluster galaxies chosen randomly. The corresponding mean power spectrum is shown in Figure 2 as Field+.1, it is the average of 4 sub-volumes. Its amplitude is higher than for the previous sample, nevertheless it lies below the simulated power spectrum of all galaxies. By increasing the fraction of galaxies in high-density regions to 50 % (sample Field+.5) the difference between the simulated sample of field and normal galaxies can be reduced further. The latter spectrum is close to the spectrum of all matter, but it has a flatter maximum.

This simple test explains qualitatively the difference observed between the power spectrum of IRAS and normal galaxies with the deficit of galaxies in high-density regions (in clusters and rich superclusters) in the former sample. It is rather difficult to calculate the correction factor to reduce such a power spectrum to the spectrum of normal galaxies. The correction factor depends on the threshold density to separate field galaxies from cluster galaxies, and on the fraction of cluster galaxies in the IRAS sample; both parameters are not known. For this reason, in the following analysis we consider the power spectrum of IRAS galaxies derived by TE95 as a representative for medium-density regions in the Universe.

### 3.3. Distribution of LCRS galaxies

The power spectrum of LCRS galaxies, according to LCRS3d, is similar to that of IRAS 1.2 Jy galaxies. It lies below the power spectrum of the APM 3-D survey of galaxies and that of the SSRS+CfA2 sample. As we have done before, we shall compare the distribution of LCRS galaxies with the distribution of superclusters. Since the details of this comparison shall be published elsewhere (Einasto et al. 1999c, hereafter E99c), here we briefly summarize the main conclusions.

As demonstrated by Einasto et al. (1994b, 1997d, hereafter EETDA and E97d, respec-

tively), very rich superclusters of galaxies form a quasi-regular network with a characteristic scale of  $120 h^{-1}$  Mpc. As shown by E99c, the LCRS slices intersect the supercluster-void network basically *in between* very rich superclusters. Only the Horologium-Reticulum supercluster crosses one of the southern strips at  $\alpha = 4^h$  and  $cz = 20,000$  km/s; the  $-39^\circ$  strip touches also the Sculptor supercluster at  $23^h 35^m$  and  $cz = 33,000$  km/s. The rest of high-density regions observed in LCRS coincide with clusters located in *poor or medium-rich* superclusters of the catalog by E97d. Thus the most of the LCRS strips only cross medium-density regions in the Universe.

The correlation function of clusters located in very rich superclusters oscillates with rather high amplitude; an oscillating correlation function corresponds to a power spectrum with a sharp turnover near the maximum (E97b, E97c). The correlation function of clusters of galaxies located in poor superclusters has a lower amplitude on large scales. The power spectrum as Fourier transformation has a flatter maximum of lower amplitude. These differences between spectra resemble those described in Section 3.1. Thus the cosmography of LCRS strips suggests that near the maximum the power spectrum of LCRS galaxies should lie *below* the power spectrum of a sample in which both rich and poor superclusters are represented. In fact, the actual power spectrum of LCRS galaxies has a lower amplitude on large scales. For this reason we shall use the LCRS power spectrum as a representative of samples which include poor and medium-rich superclusters.

On the other hand, it is possible that the low amplitude of the power spectrum is due to the very broad window function in the Fourier domain, caused by the narrowness of the LCRS survey in the declination direction (see Figure 3 of LCRS3d). The 2-D power spectrum of LCRS as derived by LCRS2d has excess power on  $100 h^{-1}$  Mpc scale. LCRS2d argue that a 2-D analysis is more sensitive to the structure on large scales than the full 3-D analysis. Then the low amplitude of the spectrum by LCRS3d could be caused by an incomplete deprojection of the 3-D power spectrum. At the present stage, we can not conclude what of the two possibilities, the different large-scale environment or problems in data analysis, is more relevant to explain the discrepancy in the power spectrum. A more detailed numerical study would be required.

### 3.4. The distribution of APM and ACO clusters of galaxies

Figure 1 shows that the maxima of the power spectra found for APM and Abell-ACO clusters of galaxies have similar amplitudes to within a factor of 1.5. However, for APM clusters the maximum occurs on larger scales. In this Section we try to clarify the reason for this difference. A catalog of APM clusters of galaxies is now published (Dalton et al. 1997).

Thus a direct comparison of the distribution of both cluster samples is possible. A detailed comparison shall be given by E99c.

The main difference between the two cluster samples is the volume they cover. The APM cluster sample is located only in the southern Galactic hemisphere, and even there it covers a much smaller area on the sky than the Abell-ACO sample. For this reason the APM cluster sample contains only a few very rich superclusters from the catalogs by EETDA and E97d, (the Pisces-Cetus, Horologium-Reticulum and Sculptor superclusters), whereas the Abell-ACO sample contains 25 very rich superclusters (E97d). These three superclusters surround one big void – the Sculptor void; in contrast, the Abell-ACO catalog contains 16 voids cataloged by EETDA and surrounded by rich superclusters. Since the Abell-ACO cluster sample covers a much larger volume in space than the APM sample (about 4 times) we can assume that the power spectrum found for the Abell-ACO clusters represents a larger sample; the power spectrum of the APM cluster sample can be considered as a local deviation. In the next Section we discuss this deviation in more detail.

#### 4. Mean galaxy power spectrum

It is our aim to determine the mean power spectrum of all galaxies in the nearby Universe. The previous analysis has shown that discrepancies exist between power spectra derived from various catalogs due to differences in the spatial distribution of objects. On the other hand, some differences may be due to differences in the data analysis technique. These are evident in the power spectra of IRAS samples as discussed above, they may be present in the spectra of LCRS galaxies. A further problem is the power spectrum reconstructed from the 2-D distribution of APM galaxies which has a much shallower turnover than the directly measured 3-D power spectrum (see Figure 1). The analysis of power spectra of simulated samples has shown that we have insufficient information to correct for all imperfections of the data analysis techniques.

For these reasons it is not realistic to determine only one mean power spectrum in the hope that it characterizes the distribution of all galaxies in the whole nearby Universe. Instead, we shall determine two mean power spectra, separately for two sets of samples (populations). In this way we try to quantify possible differences in the distribution of galaxies and in our ignorance of uncertainties in various data analysis techniques.

The first mean power spectrum was obtained from power spectra found for cluster samples and the APM 3-D, IRAS QDOT, and SSRS+CfA2 130 Mpc galaxy samples. Cluster samples cover a large volume where rich superclusters are present. We consider this popula-

tion as characteristic for high-density (HD) regions and for convenience we call it the “HD population”.

The second mean power spectrum was derived from spectra of the LCRS sample, the IRAS galaxy sample as discussed by TE95, and the APM 2-D sample. LCRS and IRAS catalogs either sample regions of the Universe characteristic for medium-rich superclusters or samples of galaxies where high-density regions are under-represented. We consider this population as characteristic for medium-density (MD) regions and call it the “MD population”. Let us remark that the differences between both spectra could be due to the differences in the populations but could also be partly an artifact of the data analysis. This could be so in the case of the APM 2-D power spectrum. The true power spectrum lies probably in between, and the uncertainty range can be understood as due to cosmic scatter (different samples) and systematic errors.

#### 4.1. Galaxy power spectrum on small scales

Observed power spectra are distorted by various effects. Coherent infall velocities to central regions of clusters and superclusters increase the amplitude of the power spectrum on all scales (Kaiser 1987). Another important effect is the relative bias caused by differences in the spatial concentration of galaxies of different absolute magnitude and morphological type to high-density regions. Luminous galaxies are mostly concentrated to central regions of groups and to clusters of galaxies. These galaxies are similar to cluster galaxies discussed above. Their power spectra are shifted to higher amplitudes; the shift is practically scale-independent (see Figure 2, GE92, Park et al. 1994, Peacock & Dodds 1994, and a detailed discussion in Paper II). On small scales 3-D galaxy spectra are distorted by peculiar velocities (Gramann et al. 1993) due to the combined influence of bulk-motions and velocity dispersion of galaxies in virialized clusters and groups.

Peacock and Dodds (1994) elaborated a technique to correct observed spectra for these effects. Here we shall apply a different approach: we accept on small scales the APM galaxy power spectrum calculated from the 2-D distribution of galaxies. The APM 2-D data is free from redshift distortions. It also has some additional advantages: as it is based on a much larger and deeper dataset, the cosmic variance is smaller than for all presently available 3-D surveys; it contains absolutely faint galaxies, thus we may assume that the amplitude of this spectrum corresponds to the amplitude of the spectrum of all galaxies.

GE92 investigated the dependence of the power spectrum on the absolute magnitude limit  $M_0$  in volume limited samples in the Local, Coma and Perseus superclusters. These

calculations show the presence of luminosity bias: if samples include only brighter galaxies ( $M_0 \leq -18.75 + 5 \log h$ ) then their power spectra have a higher amplitude. Relative bias factors (in respect to faint galaxies) for samples with luminosity limits  $M_0 = -19.75 + 5 \log h$  and  $M_0 = -20.25 + 5 \log h$  are 1.31 and 1.52, respectively. This luminosity bias has been studied since then with similar results (see dC94, Park et al. 1994, LCRS3d). On the other hand, GE92 found that fainter galaxies have no luminosity bias, i.e. within sampling errors power spectra have identical amplitudes, if the absolute magnitude limit  $M_0$  lies within the interval  $-15 + 5 \log h \geq M_0 > -18.75 + 5 \log h$ . In other words, galaxy samples with sufficiently faint absolute luminosity limits approach properties of a fair sample of the Universe (which, by definition, includes galaxies of all luminosities).

The APM 2-D sample is not a volume limited sample, but in the nearby volume it includes absolutely faint galaxies, and the amplitude of the spectrum as restored by P97 and GB98 should correspond to the sample of all galaxies. Thus we may assume that the APM 2-D sample has small or negligible absolute magnitude bias.

For these reasons we identify the power spectrum determined from de-projecting the 2-D APM data on small scales ( $k \geq 0.1 \ h \text{ Mpc}^{-1}$ ) with the mean galaxy power spectrum. We use the mean of the power spectra by P97 and GB98; the error estimates are practically identical, so we accepted the errors given by P97. On larger scales we cannot apply this power spectrum since it deviates systematically from spectra found from 3-D data.

## 4.2. Galaxy power spectrum on large scales

The main problem in calculating the mean power spectrum on larger scales is the correction for relative bias and for redshift distortions.

Redshift distortions are due to the contraction of superclusters (bulk motions) and to the velocity dispersion in virialized systems (“finger of God effect”). Bulk motions enhance the amplitude of the power spectrum on all scales and do not change the shape of the spectrum. The influence of the velocity dispersion is large on small scales where it decreases the amplitude of the spectrum. Numerical simulations by Gramann et al. (1993) and Suhhonenko & Gramann (1998) show that for realistic models the influence of velocity dispersions to the shape of the spectrum is very small for wavenumbers  $k < 0.2 \ h \text{ Mpc}^{-1}$ . Therefore, in the scales of interest we can ignore the effect of velocity dispersion. Relative bias and redshift distortion due to bulk motions both influence only the amplitude of the power spectrum. Their combined effect can be determined empirically from the comparison of amplitudes of spectra. As reference we can use the undisturbed power spectrum of the 2-D sample near the

wavenumber  $k \approx 0.1 h \text{ Mpc}^{-1}$ . Figure 1 shows that the slope of power spectra of all cluster samples is approximately the same around this scale. This observational evidence suggests that the *shapes* of 3-D power spectra in this region are not distorted by redshift effects.

Using the difference in amplitude at this wavenumber, we arrive at the following relative bias factors:  $b_{rel} = 1.30$  for SSRS+CfA2 130  $h^{-1} \text{ Mpc}$  survey (dC94), 1.12 for the APM 3-D survey (TE96), and 1.05 for the IRAS QDOT galaxy sample (P97). A high relative bias of the SSRS+CfA2 130  $h^{-1} \text{ Mpc}$  sample is expected as it consists of only bright galaxies. The difference in relative bias factors of this sample from the value found by GE92 for samples of this absolute magnitude limit (1.52) can be considered as the uncertainty of the calibration of the amplitude of the APM 2-D spectrum as characteristic for all galaxies. A low relative bias for IRAS galaxies is also expected due to arguments discussed above.

For cluster samples we find  $b_{cl} = 2.60$  (E97a) and 2.43 (R98) for Abell-ACO cluster power spectra; and  $b_{cl} = 2.24$  for the APM cluster spectrum by T98. The spatial density of APM clusters of galaxies is higher than that of Abell-ACO clusters; this means that APM clusters are defined at a lower threshold density; the power spectrum of such a sample must have a lower amplitude for reasons discussed above.

We have determined the relative bias factors around the wavenumber  $k \approx 0.1 h \text{ Mpc}^{-1}$ ; they are somewhat smaller than found by Peacock and Dodds (1994) for the whole scale interval. In using the whole scale interval Peacock & Dodds smooth the differences in the shape of power spectra of different populations. On the other hand, it is possible that the zero point of the amplitude as found by Peacock & Dodds and GE92 is closer to the true amplitude for the power spectrum for all galaxies. If this is the case then the amplitude of our adopted spectrum may be overestimated by a factor of up to  $\approx 1.15$ . This factor characterizes the possible systematic error of the amplitude of our mean power spectrum.

Applying these bias factors we normalized the power spectra of all samples to the amplitude of the APM 2-D galaxy spectrum. The results are shown in Figure 3. The power spectra were slightly smoothed and interpolated using a spline approximation for further analysis.

### 4.3. Corrections applied to observed power spectra

Our aim is to find the mean power spectrum of a large sample of the Universe as accurately as possible. In order to achieve this goal we applied a small correction to the observed spectrum in one case and investigated the deviation from a power spectrum of a larger sample in the other case.

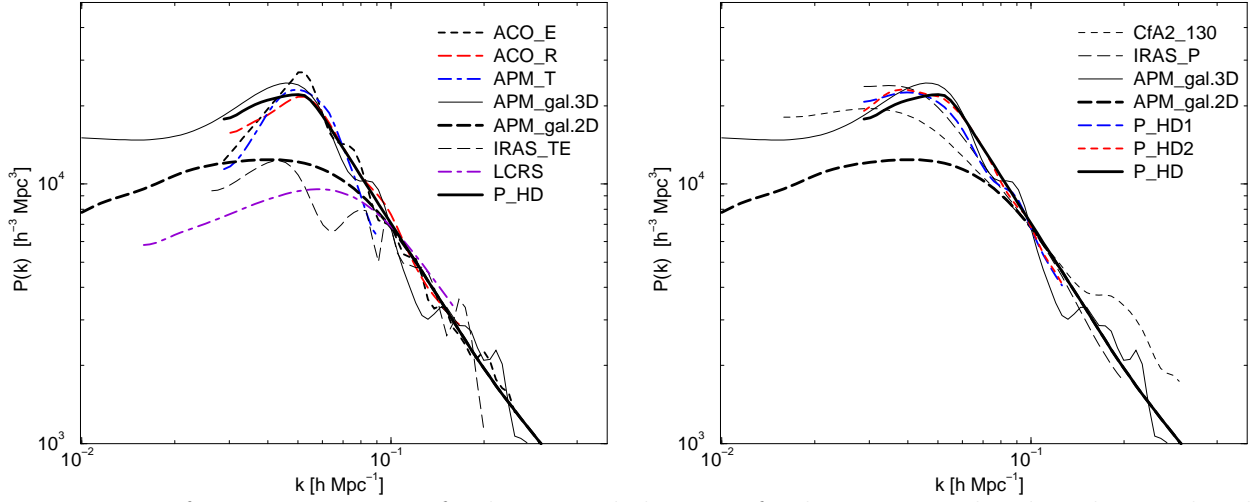


Fig. 3.— Left: Power spectra of galaxies and clusters of galaxies normalized to the amplitude of the 2-D APM galaxy power spectrum. For clarity error bars are not indicated and spectra are shown as smooth curves rather than discrete data points. Bold lines show spectra for clusters data, and designations are as in Figure 1. The spectrum for APM clusters is shifted on large scales (see text). Right: Mean power spectra derived from galaxy spectra only ( $P_{HD1}$ ); from galaxy and original cluster data ( $P_{HD2}$ ); and from galaxy and cluster data excluding APM cluster spectrum data on scale above the maximum ( $P_{HD}$ ). Random errors of the mean power spectrum at  $k = 0.05 h \text{ Mpc}^{-1}$  are 12 %, 18 %, and 12 %, respectively. Galaxy power spectra are shown for samples CfA2 130 Mpc (dC94), IRAS-P (P97), and APM 3-D (TE96). For comparison the APM galaxy spectrum derived from 2-D data is also shown; it is accepted as the mean power spectrum  $P_{MD}$ .

The first case is the power spectrum of Abell-ACO clusters of galaxies. It was determined by E97a from the cluster correlation function by Fourier transformation. This method produces an artificial local minimum of the power spectrum near the wavenumber of  $k \approx 0.035 h \text{ Mpc}^{-1}$ . The correlation function is a Fourier transformation of the power spectrum and vice versa if both statistics are determined in the whole space and do not have random and systematic errors. Actually they are determined in a limited volume and may have errors; this particular error is due to the double-conical volume where known clusters are located. A correction to this effect was applied using spectra determined for simulated clusters in N-body calculations where the true power spectrum is known (see Section 5). Figure 2a shows that after this correction the shapes of spectra of Abell-ACO clusters as determined by E97 and R98 are rather similar but not identical (see next section for a discussion of differences between samples used by E97 and R98).



The second case is the APM cluster power spectrum. The mutual separation of rich superclusters in the APM cluster sample is anomalously large. This is well seen in respective plots of clusters in E99c, and is reflected in the position of the secondary peak of the correlation function (see Figure 5 below). Rich superclusters found for Abell-ACO clusters in the same volume have also large separations. Large variations of separations of superclusters are common; similar variations are also seen on void diameters (defined by surrounding superclusters; see Table 5 of EETDA). The mean diameter of voids defined by all Abell-ACO clusters is  $91 \pm 18 h^{-1}$  Mpc, and the largest deviations reach the  $3\sigma$  level. To see how the anomalously large separation of superclusters influences the power spectrum we shifted the APM cluster spectrum on scales above the maximum towards shorter scales; the amount of the shift was determined from the difference of mean separations of rich superclusters in these catalogs. Figure 3 (left panel) shows that after this shift the power spectrum of APM clusters lies close to the spectrum of Abell-ACO clusters; in other words, the difference in power spectra of Abell-ACO and APM clusters on large scales is due to differences in the mean separation of rich superclusters. To see the effect of this peculiarity we find two mean power spectra, using the original data by T98, and ignoring the APM cluster power spectrum on scales above the maximum; results for these mean power spectra are shown in Figure 3 (right panel).

#### 4.4. Weights applied to determine the mean spectrum

After the reduction of power spectra of individual samples to the amplitude of the APM 2-D spectrum at  $k \approx 0.1 h \text{ Mpc}^{-1}$ , the remaining differences are due to random errors, errors of relative bias factors, cosmic scatter and/or problems in data sampling and reduction. In order to avoid unphysical results (negative values of the spectrum) we assume that the error distribution of the power spectrum is approximately lognormal. We calculate the weighted mean of 3-D power spectra as follows:

$$\log P(k) = \frac{\sum \log P_i(k) w_i(k)}{\sum w_i(k)} \quad (5)$$

where  $P_i(k)$  is the power spectrum of sample  $i$ , and  $w_i(k) = w_{0i}/\sigma_i^2(k)$  is the weight of the sample at  $k$ ; here  $w_{0i}$  is the mean weight of sample  $i$ , and  $\sigma_i(k)$  is the rms error of  $\log P(k)$  of sample  $i$ .

For most samples we accepted original errors, i.e. we took  $w_{0i} = 1$ . Only the weight of the power spectrum of Abell-ACO cluster sample by E97 was adjusted. E97 determined the power spectrum by Fourier transforming the correlation function, the error was calculated from the error of the correlation function (E97b, E97c). The comparison with other spectra

suggests that the error of the power spectrum by E97 is underestimated by a factor of  $\approx 1.4$ . Correcting the error of this sample we get the following relative weights of samples (in units of the weight of the APM 3-D sample; in parentheses we give the relative errors of power spectra near the maximum): 2.0 (20 %) and 1.0 (29 %) for Abell-ACO cluster samples by E97a and R98, respectively; 1.5 (23 %) for APM clusters by T98; 1.0 (29 %) for APM 3-D galaxy spectrum by TE96; 0.44 (48 %) for SSRS+CfA2 galaxy sample by dC94; and 0.88 (32 %) for the IRAS QDOT sample by P97. The mean relative error of  $P(k)$  averaged over all wavenumbers is 11 %; local deviations from this mean error are small. The volume occupied by Abell-ACO and APM cluster samples, used by E97, R98 and T98, relates approximately as 4:1.5:1; the number of clusters used is 869, 417 and 364, respectively for E97, R98 and T98 samples. In case of cluster power spectra relative weights are proportional to the number of clusters, avoiding double-counting Abell-ACO clusters used by E97 and R98.

We calculated the mean power spectrum for three sets of weights  $w_{0i}$ . In the first set we eliminated cluster samples (cluster weights were taken  $w_{0i} = 0$ ) and used only galaxy samples with their original weights; this mean power spectrum is denoted  $P_{HD1}$  in Figure 3b. In the second set we used the original power spectrum of APM clusters (with weights as described above) ( $P_{HD2}$  in Figure 3b). The third set is similar to the second one, only on scales larger than the maximum the APM cluster spectrum was ignored as it is distorted ( $P_{HD}$  in Figure 3b). The position of the maximum of the mean power spectrum for pure galaxy samples is  $k = 0.04 h \text{ Mpc}^{-1}$ ; if the APM cluster spectrum is used then the maximum of the mean spectrum is also at  $k = 0.04 h \text{ Mpc}^{-1}$ . The amplitude of the mean power spectrum on the largest scales varies within a factor of  $\approx 1.2$  for various sets; the highest amplitude has the spectrum  $P_{HD1}$  based on galaxy samples only. All variations lie well within the formal error corridor of the mean power spectrum. We see that the mean power spectrum is rather stable, it does not depend critically on the presence or absence of a particular sample.

The Abell-ACO cluster sample covers the largest volume in space. The power spectrum of APM clusters deviates on large scales with respect to the spectrum of a fair sample of the Universe for reasons discussed above. The mean spectrum based on galaxy spectra is obtained from samples covering a relatively small volume. Thus we adopt the power spectrum derived with the third set as the mean power spectrum of all galaxies; it is shown by a solid thick line in Figure 3, and is calculated for  $k \geq 0.03 h \text{ Mpc}^{-1}$ , the range for which data are available for all samples used here. For some samples, spectra are given for even larger scales, but these data are not very accurate and are ignored here (on largest scales the power spectrum is determined only by a few density waves; numerical simulations show that here the amplitude is often exaggerated, see Figure 2). This mean power spectrum corresponds to samples which include regions of all richness types, in particular very rich superclusters of galaxies; we denote this power spectrum by subscript HD (for high-density).

#### 4.5. The mean power spectrum for medium-density regions

On large and medium scales power spectra of LCRS galaxies (estimated by LCRS3d) and of IRAS samples (as analyzed by TE95) are close to the power spectrum determined from APM 2-D galaxy data. The APM 2-D power spectrum is, however, much smoother and has considerably smaller random errors than LCRS and IRAS spectra. Thus we shall use the APM 2-D power spectrum in the  $k < 0.1 h \text{ Mpc}^{-1}$  range as the characteristic spectrum for the second population.

IRAS samples as reduced by TE95 represent samples of galaxies where the number of galaxies in high-density regions is reduced. Strips of the LCRS survey essentially intersect only poor and medium-rich superclusters. As noted in the introduction to this Section, we refer to this population as “medium-rich” and denote the power spectrum with subscript MD (for medium-density). This notion is for simplicity, since it is still not clear, why the power spectrum, determined from APM 2-D data in the scale range around the maximum, is different from the power spectrum found from APM 3-D data. The amplitude of the power spectrum near the maximum is determined by the spatial distribution of very rich superclusters. It is possible that in the projection, from three to two dimensions, part of the information on the galaxy distribution is lost; in other words, the reduction of 2-D data to three dimensions is imperfect. An assessment of this and other possibilities is beyond the scope of this paper. We continue the discussion of differences between the power spectra of two populations in Section 6 using the correlation function test.

#### 4.6. Redshift and real space power spectra

The power spectrum found from APM 2-D data is given in real space by definition. We have used this spectrum in case of  $P_{MD}$  on all scales, and in case of  $P_{HD}$  on medium and small scales ( $k \geq 0.1 h \text{ Mpc}^{-1}$ ) – here both spectra are identical. On larger scales the 3-D power spectra used to find the mean spectrum for the HD population were originally determined in redshift space. We have applied the correction due to bulk motions for all observed spectra by shifting the observed spectra to match the APM spectrum. Thus our mean power spectrum is reduced from redshift space to real space. Here the assumption is that redshift distortions due to velocity dispersions within clusters and groups can be ignored on scales of interest ( $k < 0.1 h \text{ Mpc}^{-1}$ ). Numerical simulations of CDM models with cosmological constant show that on these scales redshift distortions due to velocity dispersion are small (see Fig. 2 of Gramann et al. 1993).

Figure 3 shows that the mean power spectrum,  $P_{HD}(k)$ , has a well-defined maximum

at  $k_0 = 0.050 h \text{ Mpc}^{-1}$ , an approximate power law towards smaller scales with power index  $m \approx -1.9$ , and a definite decline on scales larger than that of the maximum. The power spectrum characteristic for medium-rich regions of the Universe,  $P_{MD}(k)$ , is identical to the former spectrum over most scales, but has a flatter maximum of lower amplitude; the maximal difference in the amplitude is a factor of 2. Toward very large scales the amplitudes of both power spectra definitely decrease, the decrease being more rapid for the cluster data; the accepted mean power spectrum  $P_{HD}(k)$  is a compromise between cluster and galaxy data.

#### 4.7. Error analysis

The determination of the mean power spectra of all galaxies, found from observed power spectra of galaxies and of clusters of galaxies, involves several steps of data reduction. Here we analyze possible errors of these steps.

The main assumption in our analysis is that there exists a mean power spectrum characteristic for a population which includes all galaxies in a sufficiently large volume (fair sample). A fair sample is defined as a sample which is characteristic for all galaxies; thus, if it exists at all, it must have a power spectrum. The practical question is: do we have any evidence that real galaxy samples approach properties of a fair sample in this respect? GE92 noticed that power spectra of galaxy samples with different absolute magnitude limit are similar in shape and have identical amplitudes, if the sample is complete to sufficiently faint galaxies ( $M_0 > -18.75 + 5 \log h$ , see Section 4.1). The scatter of observed data points of power spectra for these faint galaxy samples studied by GE92 is about 10 % ( $\pm 0.05$  in  $\log P$ ) which can be attributed to the cosmic scatter as the number of galaxies in samples studied for this effect was small (from 200 to 1200). But notice that Park et al. (1994) have found a luminosity bias for all subsamples studied ( $M_0 \leq -18.5 + 5 \log h$ ), thus the lower luminosity limit of a fair sample is not yet fixed accurately.

The first step in the derivation of the mean power spectrum of galaxies is the reduction of power spectra of different galaxy and cluster samples to the spectrum of all galaxies. Here we assume that power spectra of different galaxy samples are similar in shape and differ only in the overall amplitude of the spectrum. This assumption is justified by the empirical evidence that power spectra of galaxy and cluster samples can be brought into coincidence by adjusting amplitudes of power spectra (see Figure 1 and Vogeley 1998). The coincidence is, however, not exact, and we have to estimate the corresponding error. This can be done using numerical simulations of various galaxy samples.

In a random Gaussian density field clusters of galaxies and samples of galaxies of different luminosity can be considered as samples of objects selected from the general density field by different threshold density level. Such an analysis is done in Paper II; it shows that a selection by threshold density changes the amplitude of the power spectrum (and of the correlation function), but not its shape if samples are complete in high-density regions (see also Kaiser 1984, GE92). Results of numerical simulation of galaxy samples, selected at various threshold density levels, show, that the shape of the power spectrum in real space is conserved for galaxy samples within a relative error of the order of 1 %, and in the case of cluster samples within a relative error of  $\approx 5$  %, if averaged over the scale interval  $0.01 < k \leq 1 \ h \text{ Mpc}^{-1}$  (see Table 1 of Paper II), but only 2 %, if averaged over a scale interval  $0.01 < k \leq 0.2 \ h \text{ Mpc}^{-1}$ , relevant for the present study (see Figure 2b of Paper II). As random errors of observed power spectra values (due to the cosmic scatter and to the Poisson noise) are of the order of 10 % and more (see errors shown in Figure 1), we conclude that the error introduced to the shape of the power spectrum of all galaxies by a shift in amplitude of power spectra of clusters and bright galaxies is negligible. The most serious error of the shape of the power spectrum of clusters and bright galaxies is the enhancement of the amplitude of the power spectrum on the largest scale. Such effect is observed in real samples (power spectrum of the APM 3-D galaxy sample, Figure 3) and in numerical simulations (the largest scale in model CDM6, Figure 4). For this reason we have ignored observed data points of power spectra on these largest scales.

The next aspect of the data analysis is the reduction of observed power spectra from redshift space to real space. On small scales,  $k \geq 0.1 \ h \text{ Mpc}^{-1}$ , we have accepted the mean power spectrum of galaxies on the basis of the 2-D distribution of galaxies of the APM survey, which is given in real space by construction. On larger scales we have to make a distinction between redshift distortions due to the contraction of superclusters (bulk motions) and to peculiar motion of galaxies in virialized systems. The first effect changes the amplitude of the power spectrum only, the second changes also the shape. Numerical simulations show that on scales  $k \leq 0.2 \ h \text{ Mpc}^{-1}$  the effect of peculiar motions is small for galaxies and negligible for clusters since cluster mean redshifts are used (Gramann et al. 1993, Suhhonenko & Gramann 1998). This is confirmed by direct observational data. GE92 removed peculiar motions of galaxies in groups and clusters by a special procedure; they found the galaxy power spectrum to have a power index  $n = -1.75$  in the range  $0.08 < k < 0.5 \ h \text{ Mpc}^{-1}$ . Within errors this coincides in the overlapping range of scales with the power index found by GB98 for APM galaxies, and for clusters of galaxies (E97a, R98, T97),  $n = -1.9$ . We conclude that the error of the shape of the power spectrum in real space, introduced by this reduction procedure using original spectrum data determined in the redshift space, is of the order  $\pm 0.1$  in the power index.

The main error of the amplitude correction is related to the fixing of the amplitude of the power spectrum of all galaxies in real space. We have adopted the amplitude found by P97 and GB98 from the reconstruction of the 3-D power spectrum from 2-D distribution of APM galaxies. To estimate the possible error of this normalization we have compared relative bias factors used in this study with factors found by GE92 for the nearby galaxy samples in the Local, Coma and Perseus superclusters, and by P97 for other samples. This comparison suggests that the amplitude of our mean power spectrum can have an error of up to 15 %. This normalization error is the largest possible systematic error of the power spectrum of all galaxies.

#### 4.8. Parameters of the mean galaxy power spectrum

Here we give parameters of the empirical galaxy power spectrum  $P_{HD}(k)$  for samples which include rich superclusters. We recall that by construction our power spectrum is defined in real space. The spectrum can be specified by the following parameters: the position of the maximum

$$k_0 = 0.050 \pm 0.005 \, h \, \text{Mpc}^{-1}; \quad (6)$$

the amplitude of the maximum

$$P_{HD}(k_0) = 2.30 \pm 0.25 \times 10^4 \, h^{-3} \, \text{Mpc}^3; \quad (7)$$

and the half-width of the power spectrum at the half-maximum level in the direction of increasing wavenumbers  $k$  (Eisenstein et al. 1998)

$$\text{HWHM} = 0.19 \pm 0.05 \, \text{dex}. \quad (8)$$

(Note that the full-width cannot be estimated since the observed power spectrum has yet to be determined for  $k \lesssim 0.01 \, h \, \text{Mpc}^{-1}$ ).

Another power spectrum parameter is the power index on intermediate scales ( $k_0 < k < 0.2 \, h \, \text{Mpc}^{-1}$ ), which we find to be  $m = -1.9 \pm 0.1$  for  $P_{HD}(k)$ .

The power spectrum  $P_{MD}(k)$  (i.e., for samples with poor and medium-rich superclusters) is characterized as follows: The maximum derived from APM 2-D data occurs at wavenumber  $k_0 = 0.040 \, h \, \text{Mpc}^{-1}$ , and that derived for the LCRS at  $k_0 = 0.063 \, h \, \text{Mpc}^{-1}$ ; thus, the mean value is the same as for samples including rich superclusters. The mean amplitude of the spectrum from APM 2-D and LCRS data is  $P_{MD}(k_0) = 1.19 \pm 0.27 \times 10^4 \, h^{-3} \, \text{Mpc}^3$ . Formal errors are approximately the same as for samples which include rich superclusters. Since the power spectrum for these samples is flatter, the half-width of the power spectrum on half-maximum level is much larger:  $\text{HWHM} = 0.42 \pm 0.10 \, \text{dex}$ . The power index on intermediate

scales is the same as for the previous case, only it holds for a smaller range in  $k$ -space (see Figure 3).

Error estimates given above are determined from the mean errors of the power spectra of individual samples used. These sampling errors are comparable to the possible systematic error of the amplitude due to normalization, discussed above. The overall error of the amplitude of the mean power spectrum of galaxies (sampling + systematic errors) is about 20 %.

The reason why there exist two populations of galaxies in the local Universe with different clustering properties and power spectra is not fully clear. The comparison of power spectra and correlation functions of clusters of galaxies in superclusters of different richness (E97b, E97c) hints at the possibility that we simply are dealing with regions of different size. Very rich superclusters are rare; so, whereas larger samples include the rarer, richer superclusters, in smaller samples only medium and poor superclusters are present. If this assumption is correct, we can consider our Abell-ACO cluster sample as the closest to a fair sample of the Universe. But this needs verification from much deeper and larger galaxy samples.

Table 2 contains tabulated values of the mean galaxy power spectrum  $\log P_{gal}(k)$ , found for samples including rich superclusters. The wavenumber  $k$  and the spectrum are given in usual units as described above; to allow the use of the power spectrum to calculate Fourier integrals data are given with a small step,  $\Delta \log k = 0.02$ ;  $\epsilon$  is the error of the logarithm of the power spectrum, calculated from errors of individual determinations of the spectrum;  $n$  is the power index found for interval  $(i - 1) - i$  ( $i$  is the row number). We give also the mean linear matter power spectrum,  $\log P_{lin}$ , found in Papers II and III of this series, and its power index  $n$ ; they are also found for the power spectrum characteristic for high-density regions. Small waves of the linear power spectrum are due to Doppler oscillations of the transfer function, used to calculate theoretical power spectra applied for the extrapolation on small scales (for details see Paper III). The mean power spectrum for medium-density regions,  $P_{MD}(k)$ , is accepted in accordance with P97 and GB98, and is not tabulated here.

## 5. The correlation function test

In this Section we shall use various determinations of the correlation function of galaxies and clusters of galaxies to check the consistency of our power spectra. The correlation function and the power spectrum are mutually related via Fourier transformation. In the absence of random and systematic errors the observed correlation function should be identical

to the Fourier transformation of the observed spectrum and vice versa, when known over the full range of  $k$  and  $r$ . The actual situation is different. Both functions are measured in a limited range of scales; and various selection effects influence the correlation function and the power spectrum in different ways. For this reason the correlation function and the power spectrum provide two complementary methods for characterizing the large-scale structure of the Universe.

Of special interest is the correlation function for large separations, since it is very sensitive to the shape of the power spectrum near its maximum. In this region differences between various samples are more pronounced. Also, of particular interest is the correlation function of clusters of galaxies in rich and very rich superclusters since its amplitude is larger (E97b, E97c).

### 5.1. Simulated correlation functions

Let us first analyze the relation between the correlation function and the power spectrum of matter and of clusters of galaxies in simulated rich superclusters. Our purpose is to clarify how well high-density regions, in particular very rich superclusters, characterize the distribution of matter in general. For this purpose we perform 3-D N-body simulations. Table 1 summarizes the main parameters of our models which differ basically in the behavior around the maximum of the spectrum. The “DPS” model is the double-power law model with sharp transition, eqn. (3), with parameters:  $n = 1$ ;  $m = -1.5$ ; and  $k_0 = 0.05 h \text{ Mpc}^{-1}$ . The “DPP” model is similar to the previous one, but its power spectrum has an additional peak of relative amplitude  $\approx 1.7$  near the maximum. The other two models are the standard CDM model and a flat model with cosmological constant, designated as CDM1 and CDM2, respectively. The length of the simulation box was taken to be  $L = 6\lambda_0$ , where  $\lambda_0 = 2\pi/k_0$ ; for the above transition scale this gives  $L = 720 h^{-1} \text{ Mpc}$ . Calculations were performed with a PM code with  $256^3$  cells and  $128^3$  particles, the present epoch was identified by rms density fluctuations within the simulation cell of size  $l = L/256 = 2.8 h^{-1} \text{ Mpc}$ . The rms amplitude of density perturbations of dark matter is characterized by the  $\sigma_8$  parameter; it was calculated from the power spectrum of matter by integration (see Paper II).

Clusters of galaxies were identified with a tree code which picks up high-density clumps of particles. Parameters of the neighborhood search were chosen so as to obtain a total of  $2 \times 10^4$  clusters in each model. From this initial cluster sample a subsample was selected choosing the  $N_{cl} \approx 9300$  most massive candidates (the mass is determined from the number of particles included). This corresponds to the spatial density of Abell-ACO clusters of  $n = 2.5 \times 10^{-5} h^{-3} \text{ Mpc}^3$  in this volume, taking into account the selection function of real



clusters both in galactic latitude and distance (see E97b and E97d for details).

These simulations have a low spatial resolution. To check how sensitive the clustering properties are to the chosen resolution, we calculated a new variant (CDM6, with much higher resolution) for the standard CDM model. This model was calculated with a different algorithm and different realization of the initial density field; it has a lower  $\sigma_8$  value, thus its amplitude is lower. The lower mass limit of clusters is also different since the rate of cluster formation depends on the amplitude of the power spectrum on large scales.

Matter power spectra derived from all test particles are shown in the upper panel of Figure 4. As indicated by the  $\sigma_8$  value, the model CDM6 has a spectrum of lower amplitude. In the present context the absolute normalization of the amplitude of the power spectrum is of minor importance as we compare cluster correlation functions for the same model, calculated directly from simulated cluster samples and indirectly from the Fourier transformation of the matter power spectrum. On large scales the power spectrum of the CDM6 model is rising, which is probably a numerical artifact (similar deviations occur if we extract from the whole simulation box a smaller sub-volume and find the power spectrum there).

These spectra were used to calculate the correlation function of matter using the Fourier transformation. As demonstrated already by Kaiser (1984), the correlation function of clusters of galaxies has a higher amplitude than the correlation function of galaxies. The same is true for power spectra. The analysis by E97b and E97c has shown that the amplitude of the correlation functions (and of the power spectra) of clusters in very rich superclusters

Table 1: Simulation parameters

| Model | Number<br>of particles | Number<br>of cells | $L_{box}$<br>( $h^{-1}$ Mpc) | $\Omega_0$ | $\Omega_\Lambda$ | $h$ | $\sigma_8$ | $N_{cl}$ |
|-------|------------------------|--------------------|------------------------------|------------|------------------|-----|------------|----------|
| CDM1  | $128^3$                | $256^3$            | 720                          | 1.0        | 0.0              | 0.5 | 0.57       | 9350     |
| CDM2  | $128^3$                | $256^3$            | 720                          | 0.2        | 0.8              | 0.5 | 0.79       | 9373     |
| DPS   | $128^3$                | $256^3$            | 720                          | 1.0        | 0.0              | 0.5 | 0.88       | 9339     |
| DPP   | $128^3$                | $256^3$            | 720                          | 1.0        | 0.0              | 0.5 | 0.79       | 9445     |
| CDM6  | $240^3$                | $720^3$            | 720                          | 1.0        | 0.0              | 0.5 | 0.46       | 9329     |

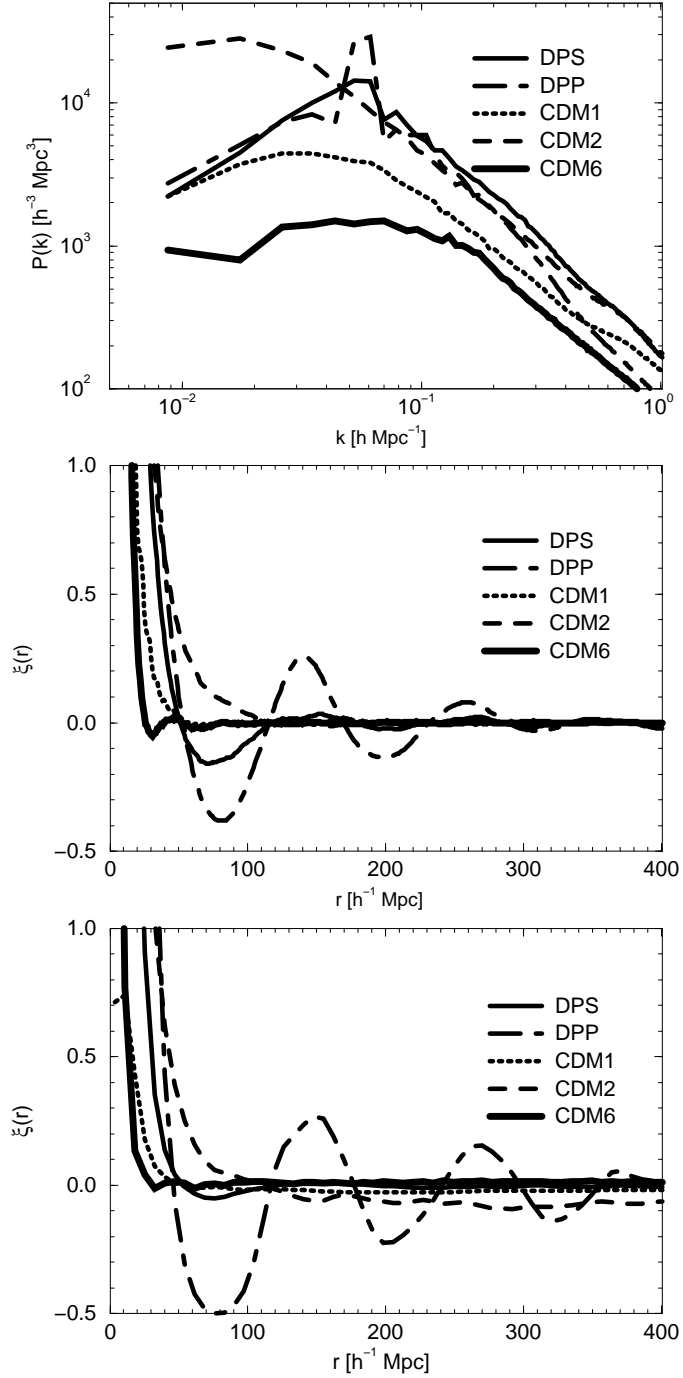


Fig. 4.— Spectra and correlation functions of N-body models. Upper panel: matter spectra; middle panel: correlation functions calculated from matter spectra by Fourier transformation and enhanced in amplitude to simulate cluster correlation functions; lower panel: actual correlation functions of model clusters in rich superclusters. Models are designated as in Table 1.

is larger than that for galaxies, by a factor of about 50, which corresponds to a relative bias factor of 7. Thus, in order to find the expected correlation function of clusters in very rich superclusters, we multiply the matter correlation functions of our models by this factor (here we ignore the difference between the matter and galaxy power spectra and correlation functions as this difference is small, see below). The resulting expected correlation functions are plotted in the middle panel of Figure 4.

Using model cluster catalogs we constructed model superclusters applying a procedure identical to the determination of real superclusters (EETDA, E97d). The correlation functions of clusters of galaxies located in very rich superclusters with 8 or more members are shown in the lower panel of Figure 4. We see that these correlation functions are rather similar to expected correlation functions calculated from the distribution of all particles by Fourier transforming the matter power spectra.

We conclude that simulated superclusters, in particular very rich superclusters, can be used to describe the matter distribution of the whole model. A check with high-resolution simulation CDM6 confirms results obtained with medium resolution. In all CDM models the distribution of superclusters is much less regular than in DPS and especially in DPP model. These geometric properties are well expressed through the correlation functions and power spectra of respective models (for the geometric interpretation of correlation functions see E97b, E97c). Thus we may hope that the correlation function of real rich superclusters can be used to test the distribution of the whole matter in the Universe. In particular, we note that the correlation function is very sensitive to the shape of the power spectrum around the maximum. The correlation function is oscillating only in the case when the power spectrum has a sharp peak at the maximum, otherwise it approaches the zero level on large scales.

A similar conclusion has been obtained by Suhhonenko and Gramann (1998) using high-resolution N-body simulations and analytical calculations based on the Press-Schechter (1974) algorithm.

## 5.2. Observed correlation functions

Now we compare the correlation function for clusters in very rich superclusters as derived from Abell-ACO clusters with that from APM clusters (E97b, E99c). As can be seen in the left panel of Figure 5, our data show clearly that the correlation function of clusters in very rich superclusters has a well-defined secondary maximum for both cluster samples. The secondary maximum of the cluster correlation function is due to the correlation of clusters across large voids. The mutual separation of very rich superclusters of the APM

cluster sample is rather large. This separation determines the location of the secondary maximum of the correlation function, which is  $185 h^{-1}$  Mpc, determined both from the APM cluster sample, and from the Abell-ACO cluster sample in the same volume. The secondary maximum of the correlation function for the whole Abell-ACO cluster sample is located at a separation of  $140 h^{-1}$  Mpc. The amplitude of the secondary maximum for APM clusters is exaggerated since the sample is small. In a small sample the number of rich superclusters is small (APM sample contains only 3 very rich superclusters); the secondary maximum of the correlation function is given by the mutual separation of these few superclusters. In a large sample there are many rich superclusters, all of them have different separations. Local secondary maxima of the correlation function (found in small subvolumes) cancel each other partly out, and the secondary maximum of the mean correlation function calculated for the whole volume has a much lower amplitude than maxima in smaller subvolumes.

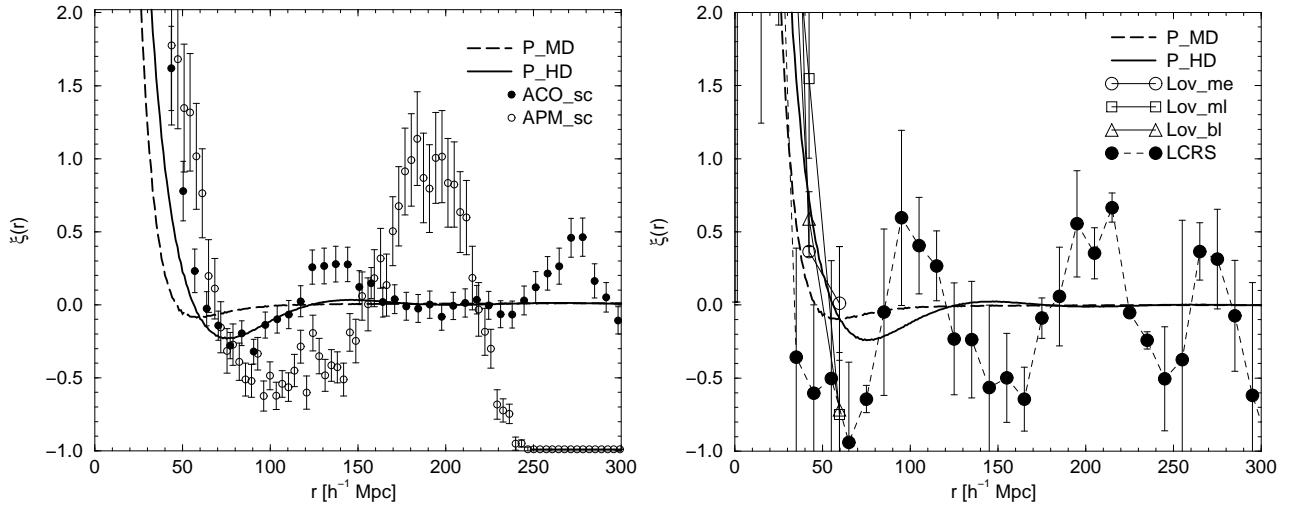


Fig. 5.— The correlation functions of galaxies and clusters of galaxies. The left panel gives these functions for clusters of galaxies located in very rich superclusters of Abell-ACO and APM samples. The right panel shows the correlation functions of galaxies in the APM 3-D “1-in-20” sample (Loveday et al. 1995) and LCRS sample (Tucker et al. 1997); Lov-me, Lov-ml, Lov-bl denote medium-bright early type, medium-bright late type, and bright late type galaxies from Figure 6 of Loveday et al. . For comparison we show the correlation functions calculated by Fourier transformation of power spectra,  $P_{HD}(k)$  (bold solid line), and  $P_{MD}(k)$  (bold dashed line). All galaxy correlation functions are enhanced in amplitude to match the correlation functions for clusters in rich superclusters.

The location of the secondary maximum of the correlation function is closely connected with the position of the maximum of the power spectrum (E97b, E97c). As both the spectrum and the correlation function of the APM cluster sample are determined from a much smaller

volume than those for the Abell-ACO sample, we have to conclude that the differences in the power spectrum and the correlation function derived for these two cluster samples are due to cosmic fluctuations.

In Figure 5 we also give the correlation functions calculated from the observed power spectrum of matter,  $P_{HD}(k)$ , as adopted in the previous Section, as well as from the spectrum  $P_{MD}(k)$  which has a flat maximum. These functions were also matched in amplitude to that of the cluster correlation function in rich superclusters. The correlation function calculated from the power spectrum  $P_{HD}(k)$  has a zero crossing at  $60 h^{-1}$  Mpc, not far from the zero crossing of the correlation function of clusters in Abell-ACO ( $60 h^{-1}$  Mpc) and APM ( $70 h^{-1}$  Mpc) rich superclusters. On smaller separations its amplitude is lower than the observed cluster correlation amplitude. The correlation function derived from the power spectrum  $P_{MD}(k)$  has a much lower zero crossing (about  $45 h^{-1}$  Mpc) and amplitude on small scales.

Cluster correlation functions can be compared with galaxy correlation functions derived by Loveday et al. (1995) for the APM “1-in-20” redshift survey and for LCRS galaxies (Tucker et al. 1997), as indicated in the right panel of Figure 5. Unfortunately, Loveday et al. calculated the galaxy correlation functions only for  $r \leq 60 h^{-1}$  Mpc, so that the presence or absence of a secondary maximum of the galaxy correlation function cannot be established. For the present comparison the position of zero crossing is important, as it does not depend on the relative bias factor. For various subsamples of the APM galaxy sample the zero crossing lies between  $50$  and  $55 h^{-1}$  Mpc, a bit less than for the correlation function derived from the power spectrum  $P_{HD}(k)$  ( $60 h^{-1}$  Mpc). The correlation function of galaxies in the LCRS galaxies (Tucker et al. 1997) has a zero crossing ( $32 h^{-1}$  Mpc) not far from that of the correlation function derived from the power spectrum  $P_{MD}(k)$  ( $45 h^{-1}$  Mpc). Note also that the correlation function of LCRS galaxies is oscillating as the cluster correlation function. The period of oscillations is approximately  $100 h^{-1}$  Mpc, as expected from the position of the maximum of the power spectrum of LCRS galaxies, and from the separation of rich galaxy filaments in LCRS slices. We see that correlation functions are in satisfactory agreement with power spectra.

We conclude that the correlation function test reinforces our findings on the basis of the power spectra. There exist differences in clustering properties of populations in the nearby Universe. One population is characteristic for rich superclusters, and the other for poorer ones. The former population has a power spectrum with a sharp peak and a correlation function with zero crossing near  $60 h^{-1}$  Mpc, the latter population has a flatter power spectrum and a zero crossing of the correlation function near  $40 h^{-1}$  Mpc. On the other hand, all power spectra of samples of the MD population have one or other problem – either

with limitations inherent to the dataset itself or with the appropriateness of the data analysis. Thus, the differences between our adopted mean power spectra of high and medium density regions could be partly attributed to these problems.

## 6. Conclusions

In this paper our goal is to determine the mean power spectrum of galaxies in real space in a large representative volume. Our principal assumption is that a fair sample has a power spectrum, i.e. a mean spectrum characteristic for a population which includes all galaxies including faint dwarf galaxies.

We have used observed power spectra determined from deep galaxy and cluster samples. In analyzing these samples we have found two distinct populations. The first population is characteristic of volumes containing superclusters of a wide variety of richness classes; samples which can be identified with this first population include the Abell-ACO and the APM cluster catalogs, the 3-D redshift survey of APM galaxies, and the SSRS+CfA2 130 Mpc galaxy catalog. The second population is characteristic of volumes which – due to smaller volume and/or unfortunate survey geometry – lack the rarer, richer superclusters; this “medium-rich” population is represented by the LCRS (whose slice geometry seems to be anti-correlated with the positions of the richest superclusters) and the IRAS galaxy sample (since IRAS galaxies tend to avoid high-density environments).

We have found mean power spectra for these populations. Mean power spectra were reduced to correct for redshift distortions due to bulk motions. On medium and small scales the power spectra of the two populations are identical. This is because on these scales, the mean power spectrum is adopted from 3-dimensional reconstruction of the 2-dimensional distribution of APM galaxies, which is free of redshift distortions and, due to the very large size of the sample, has a small cosmic scatter.

On large scales, the mean power spectrum which we adopted for the high-density population,  $P_{HD}(k)$ , was derived from observed power spectra in redshift space for cluster and galaxy samples listed above. Redshift space spectra are reduced to real space and corrected for the relative bias. On these scales redshift distortions due to peculiar motions of galaxies in clusters and groups are small and can be ignored. The mean power spectrum has a fairly sharp maximum at  $k = 0.05 \pm 0.01 \ h \text{ Mpc}^{-1}$ , and a half-width half-maximum of  $\text{HWHM} = 0.19 \pm 0.05 \text{ dex}$ ; on smaller scales, it exhibits an almost exact power law of index  $n = -1.9$ . Clusters of galaxies have the largest weight in the determination of this power spectrum.

The power spectrum we find for medium-density regions,  $P_{MD}(k)$ , has a flatter maximum with  $\text{HWHM} = 0.42 \pm 0.10$  dex.

We have argued that clusters of galaxies adequately trace the true mass distribution in the Universe, so that the cluster data based power spectrum of galaxies can probably be considered as the power spectrum of a fair sample of the Universe.

*Acknowledgements:* We thank E. Gaztañaga, H. Tadros, and M. Vogeley for supplying the Tartu group with the numerical values of galaxy and cluster power spectra, and M. Gramann and A. Szalay for discussion. We thank the referee, M. Vogeley, for constructive criticism. This work was supported by the Estonian Science Foundation (grant 2625), International Science Foundation (grant LLF100). JE and AS were supported by the Deutsche Forschungsgemeinschaft in Potsdam; AS was partially supported by the Russian Foundation for Basic Research under Grant 96-02-17591; RC was supported by grants NAG5-2759, AST9318185; HA benefitted from financial support by CONACYT (Mexico; Cátedra Patrimonial, ref 950093).

## REFERENCES

- Abell, G. 1958, ApJS, 3, 211
- Abell, G., Corwin, H. & Olowin, R. 1989, ApJS, 70, 1 (ACO)
- Broadhurst, T.J., Ellis, R.S., Koo, D.C., & Szalay, A.S. 1990, Nature, 343, 726
- Cen, R., & Ostriker, J.P. 1992, ApJ, 399, L113
- Cen, R., & Ostriker, J.P. 1998 (in preparation)
- da Costa, L.N., Vogeley, M.S., Geller, M.J., Huchra, J.P., and Park, C. 1994, ApJ, 437, L1 (dC94)
- Dalton, G.B., Maddox, S.J., Sutherland, W.J., & Efstathiou, G. 1997, MNRAS, 289, 263
- Einasto, J., Einasto, M., Gottlöber, S., Müller, V., Saar, V., Starobinsky, A.A., Tago, E., Tucker, D., Andernach, H., & Frisch, P. 1997a, Nature, 385, 139 (E97a)
- Einasto, J., Einasto, M., Frisch, P., Gottlöber, S., Müller, V., Saar, V., Starobinsky, A.A., Tago, E., & Tucker, D. & Andernach, H. 1997b, MNRAS, 289, 801 (E97b)
- Einasto, J., Einasto, M., Frisch, P., Gottlöber, S., Müller, V., Saar, V., Starobinsky, A.A., Tago, E., & Tucker, D. 1997c, MNRAS, 289, 813 (E97c)

- Einasto, J., Einasto, M., Tago, E., Müller, V., Knebe, A., Cen, R., Starobinsky, A.A. & Atrio-Barandela, F. 1999a, ApJ (in press) (Paper II)
- Einasto, J., Einasto, M., Tago, E., Starobinsky, A.A., Atrio-Barandela, F., Müller, V., Knebe, A. & Cen, R. 1999b, ApJ (in press) (Paper III)
- Einasto, J., Klypin, A.A., Saar, E. & Shandarin, S.F. 1984, MNRAS, 206, 529
- Einasto, J., Saar, E., Einasto, M. Freudling, W., & Gramann, M. 1994a, ApJ, 429, 465 (E94)
- Einasto, M. 1991, MNRAS, 252, 261
- Einasto, M., Einasto, J., Tago, E., Dalton, G., & Andernach, H. 1994b, MNRAS, 269, 301 (EETDA)
- Einasto, M., Einasto, J., Tago, E., Tucker, D., & Andernach, H. 1999c (in preparation) (E99c)
- Einasto, M., Tago, E., Jaaniste, J., Einasto, J., & Andernach, H. 1997d, A&AS, 123, 119 (E97d)
- Eisenstein, D.J., Hu, W., Silk, J., & Szalay, A.S. 1998, ApJ, 494, L1 [astro-ph/9710303]
- Frisch, P., Einasto, J., Einasto, M., Freudling, W., Fricke, K.J., Gramann, M., Saar, V., & Toomet, O. 1995, A&A, 296, 611
- Gaztañaga, E. & Baugh, C.M. 1998, MNRAS, 294, 229 (GB98)
- Gramann, M., Einasto, J. 1992, MNRAS, 254, 453 (GE92)
- Gramann, M., Cen, R. & Bahcall, N.A. 1993, ApJ, 419, 440
- Hoyle, F., Baugh, C.M., Shanks, T., & Ratcliffe, A. 1998, MNRAS (in press) [astro-ph/9812135]
- Kaiser, N. 1984, ApJ, 284, L9
- Kaiser, N. 1987, MNRAS, 227, 1
- Landy, S.D., Shectman, S.A., Lin, H., Kirshner, R.P., Oemler, A.A., & Tucker, D. 1996, ApJ, 456, L1 (LCRS2d)
- Lin, H., Kirshner, R.P., Shectman, S.A., Landy, S.D., Oemler, A., Tucker, D.L., & Schechter, P.L. 1996, ApJ 471, 617 (LCRS3d)
- Loveday, J., Maddox, S.J., Efstathiou, G., & Peterson, B.A. 1995, ApJ, 442, 457



- Maddox, S.J., Efstathiou, G., & Sutherland, W.J. 1996, MNRAS, 283, 1227
- Park, C., Vogeley, M. S., Geller, M. J., & Huchra, J. P. 1994, ApJ, 431, 569
- Peacock, J.A. 1997, MNRAS, 284, 885 (P97)
- Peacock, J.A. & Dodds, S.J. 1994, MNRAS, 267, 1020
- Press, W.H. & Schechter, P.L. 1974, ApJ, 187, 425
- Retzlaff, J., Borgani, S., Gottlöber, S., Klypin, A., & Müller, V. 1998, NewA (submitted), [astro-ph/9709044] (R98)
- Saunders, W., Rowan-Robinson, M. & Lawrence, A. 1992, MNRAS, 258, 134
- Suhhonenko, I., & Gramann, M. 1998, ApJ (submitted)
- Tadros, H., & Efstathiou, G. 1995, MNRAS, 276, L45 (TE95)
- Tadros, H., & Efstathiou, G. 1996, MNRAS, 282, 1381 (TE96)
- Tadros, H., Efstathiou, G. & Dalton, G. 1998, MNRAS, 296, 995 [astro-ph/9708259] (T98)
- Tucker, D. L., Oemler, A., Jr., Kirshner, R. P., Lin, H., Shectman, S.A., Landy, S.D., Schechter, P.L., Müller, V., Gottlöber, S. & Einasto, J. 1997, MNRAS, 285, 5
- Vogeley, M. 1998, The Evolving Universe, ed. D. Hamilton, (Dordrecht: Kluwer), p. 395 [astro-ph/9805160]
- Vogeley, M., Park, C., Geller, M.J. & Huchra, J.P. 1992, ApJ, 391, L5

Table 2: Power spectra

[illegible]

| $\log k$ | $\log P_{gal}$ | $\epsilon$ | $n$   | $\log P_{lin}$ | $n$   |
|----------|----------------|------------|-------|----------------|-------|
| .22      | 2.0735         | .0417      | -1.33 | .7845          | -2.46 |
| .24      | 2.0464         | .0407      | -1.35 | .7352          | -2.46 |
| .26      | 2.0189         | .0397      | -1.38 | .6860          | -2.46 |
| .28      | 1.9909         | .0387      | -1.40 | .6368          | -2.46 |
| .30      | 1.9625         | .0377      | -1.42 | .5876          | -2.46 |
| .32      | 1.9339         | .0367      | -1.43 | .5384          | -2.46 |
| .34      | 1.9050         | .0357      | -1.44 | .4891          | -2.46 |
| .36      | 1.8760         | .0347      | -1.45 | .4399          | -2.46 |
| .38      | 1.8470         | .0338      | -1.45 | .3907          | -2.46 |
| .40      | 1.8180         | .0329      | -1.45 | .3414          | -2.46 |
| .42      | 1.7891         | .0320      | -1.45 | .2922          | -2.46 |
| .44      | 1.7603         | .0312      | -1.44 | .2430          | -2.46 |
| .46      | 1.7316         | .0304      | -1.43 | .1938          | -2.46 |
| .48      | 1.7031         | .0297      | -1.43 | .1446          | -2.46 |
| .50      | 1.6747         | .0289      | -1.42 | .0954          | -2.46 |
| .52      | 1.6465         | .0283      | -1.41 | .0462          | -2.46 |
| .54      | 1.6184         | .0276      | -1.40 | -.0030         | -2.46 |
| .56      | 1.5904         | .0269      | -1.40 | -.0522         | -2.46 |
| .58      | 1.5625         | .0263      | -1.39 | -.1014         | -2.46 |
| .60      | 1.5346         | .0257      | -1.40 | -.1507         | -2.46 |
| .62      | 1.5066         | .0251      | -1.40 | -.2000         | -2.47 |
| .64      | 1.4785         | .0246      | -1.41 | -.2494         | -2.47 |
| .66      | 1.4501         | .0240      | -1.42 | -.2987         | -2.47 |
| .68      | 1.4214         | .0235      | -1.44 | -.3481         | -2.47 |
| .70      | 1.3923         | .0231      | -1.45 | -.3976         | -2.47 |
| .72      | 1.3632         | .0226      | -1.46 | -.4470         | -2.47 |
| .74      | 1.3342         | .0222      | -1.45 | -.4964         | -2.47 |
| .76      | 1.3054         | .0217      | -1.44 | -.5459         | -2.47 |
| .78      | 1.2771         | .0214      | -1.42 | -.5953         | -2.47 |
| .80      | 1.2493         | .0210      | -1.39 | -.6449         | -2.48 |
| .82      | 1.2223         | .0207      | -1.35 | -.6945         | -2.48 |
| .84      | 1.1959         | .0204      | -1.32 | -.7442         | -2.49 |
| .86      | 1.1694         | .0202      | -1.33 | -.7938         | -2.48 |
| .88      | 1.1422         | .0200      | -1.36 | -.8433         | -2.47 |
| .90      | 1.1135         | .0197      | -1.43 | -.8934         | -2.51 |
| .92      | 1.0829         | .0195      | -1.53 | -.9444         | -2.55 |
| .94      | 1.0496         | .0192      | -1.67 | -.9935         | -2.46 |
| .96      | 1.0130         | .0189      | -1.83 | -1.0391        | -2.28 |
| .98      | .9744          | .0186      | -1.93 | -1.0895        | -2.52 |
| 1.00     | .9363          | .0183      | -1.91 | -1.1544        | -3.24 |